COMPOSITIONAL TERRANES ON MERCURY DERIVED FROM MEASUREMENTS OF FAST NEUTRONS. David J. Lawrence[1], Patrick N. Peplowski[1], Andrew W. Beck[1], William C. Feldman[2], Elizabeth A. Frank[3], Timothy J. McCoy[4], Larry R. Nittler[3], Nancy L. Chabot[1], Carolyn M. Ernst[1], Sean C. Solomon[3,5]; [1]Johns Hopkins University Applied Physics Laboratory, Laurel, MD 20723, USA (David.J.Lawrence@jhuapl.edu); [2]Planetary Science Institute, Tucson, AZ 85719, USA; [3]Carnegie Institution of Washington, Washington, DC 20015, USA; [4]Smithsonian Institution, Washington, DC 20560, USA; [5]Lamont-Doherty Earth Observatory, Columbia University, Palisades, NY 10964, USA.

Introduction: One of the primary goals of the MErcury Surface, Space ENvironment, GEochemistry, and Ranging (MESSENGER) mission was to measure the surface elemental composition of Mercury in order to improve our understanding of the planet's formation and geological history. Data from the X-Ray Spectrometer (XRS) and Gamma-Ray and Neutron Spectrometer (GRNS) have provided elemental abundances for H, K, Th, and U and the elemental weight-fraction ratios Na/Si, Mg/Si, Al/Si, S/Si, Cl/Si, Ca/Si, Ti/Si, Cr/Si, Mn/Si, and Fe/Si [1-12]. Slow-neutron measurements from the anticoincidence shield of the Gamma-Ray Spectrometer (GRS) portion of the GRNS have provided spatially resolved measurements of thermal-neutron-absorbing elements [13]. These data have demonstrated that Mercury has an iron-poor crust, its surface is not depleted in volatile elements (e.g., Na, K, Cl, and S), it has compositional terranes with clear boundaries, and its geochemical diversity is likely dominated by Mg-rich minerals [14].

Despite this large amount of compositional information, the existing elemental abundance datasets have substantial limitations, such as uneven coverage for some elements and a range of element-dependent uncertainties. Composition information that is independent of the limitations of prior measurements provides useful constraints on the bulk composition of Mercury's surface. Here, we present an analysis of fast neutrons at Mercury that provide new, independent information on Mercury's surface composition.

Planetary Fast Neutrons: Planetary fast neutrons are produced by galactic cosmic-ray (GCR) interactions with the surfaces of airless planetary bodies [15]. For planetary surfaces that have small amounts (less than a few hundred parts per million) of bulk hydrogen (H), fast neutrons provide a measure of the average atomic mass (<A>). With particle transport codes that have been validated from other planetary studies [16], we have calculated fast-neutron fluxes from elemental compositions for different Mercury compositional terranes (Figure 1). The model-based fluxes confirm that the relative fast-neutron flux for Mercury is proportional to <A>, as is the case for the Moon [15] and asteroid Vesta [16]. A map of fast neutrons for Mercury should therefore provide a measure of <A> across Mercury's surface.

Fast Neutrons at Mercury: The MESSENGER mission ended operations on 30 April 2015 when the spacecraft impacted the planet after over four years in orbit. During orbital operations, fast-neutron data were collected from the MESSENGER Neutron Spectrometer (NS), which was operated nearly continuously from

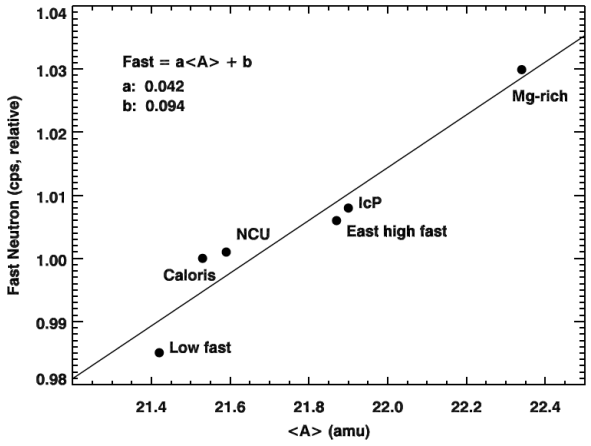

Fig. 1. Calculated fast-neutron count rates, in counts per second (cps) relative to the mean modeled count rates, for different values of <A>. The different <A> values were determined from XRS and GRS elemental compositions selected at different locations on Mercury. The compositions were determined from the regions shown in Figure 3. NCU: northern composition unit. IcP: intercrater plains.

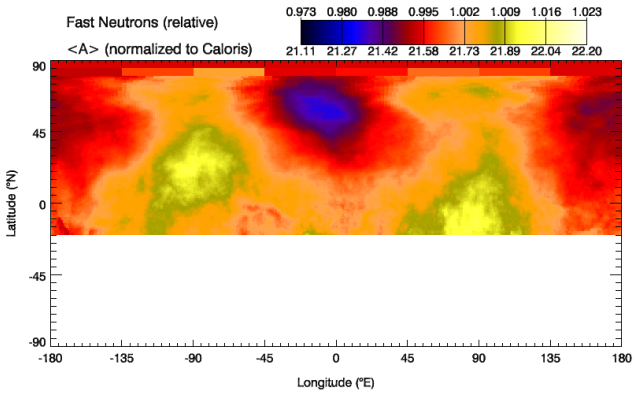

Fig. 2. Map of fast-neutron count rates on Mercury relative to the mean value. The scale bar is given in units of relative count rates and <A>, where the <A> values are normalized to those inferred within the Caloris basin (32ºN, 162ºE) from mapped XRS and GRS compositional data.

orbit. In comparison with the published fast-neutron data on variations with latitude [3], here we have sufficient data to derive a map of fast-neutron variations across Mercury's surface (Figure 2). The data-reduction procedures used to derive this map were based on previous analyses of neutron data from Mercury [3,13]. The map was derived from 82,962 individual measurements of fast-neutron count rates after selections were made to optimize near-planet data (<1500 km altitude) and viewing-geometry look directions. The final map was derived with an altitude-dependent smoothing algorithm to increase the mapped ratio of signal to noise and account for the variable spatial footprint.

The measured count rates have a dynamic range of 3%. From a comparison with modeled count rates, most of this variability is due to compositional variations across Mercury's surface. In comparison with similar measurements at the Moon and Vesta, Mercury has by far the smallest dynamic range in fast neutrons, versus those at the Moon and Vesta of 30% and 6%, respectively [15,16].

From four compositional groupings identified in the fast-neutron map, we constructed a fast-neutron map of compositional terranes (Figure 3). Comparing our results to prior geochemical terrane data, we find that: (1) The high-Mg terrane, originally identified from XRS-derived Mg/Si ratios, is also seen in fast neutrons. (2) Fast neutrons delineate a terrane that includes the Caloris exterior (CE) plains and Caloris basin (CB) interior plains. In prior terrane identification, CB was distinctive but CE more closely resembled a composition similar to the mean for Mercury. Fast-neutron data show that, for CB, lower values of Fe, S, and neutron-absorbing elements [10,13] are likely compensated by higher concentrations of other elements to yield an overall value of <A> that is similar to that for CE. (3) A high-<A> region located in the eastern equatorial region, which had been suggested in the XRS composition maps, is clearly delineated by the fast neutrons. (4) The fast-neutron data delineate a geochemical terrane that has a lower flux of fast neutrons than average ("low-fast region"). The fast-neutron data show that this region lies mostly within the northern volcanic plains but is not delineated precisely by the plains boundaries. Additional evidence for the existence of a separate geochemical terrane in this region comes from K concentrations [7], which show a notable decrease of K in approximately the same location as the low-fast region.

A comparison of the fast-neutron data with MESSENGER photogeological mapping [18] shows that the low-fast region is located almost entirely within western ejecta of Hokusai crater (17ºE, 58ºN) (Fig. 4). Hokusai is the youngest large crater on Mercury, and its prominent rays of ejecta stretch almost completely around the planet. These results show that the northern parts of Hokusai ejecta are compositionally distinct. Additional studies of other compositional data (slow neutrons, mapped epithermal neutrons) should provide additional information regarding the nature and source of this distinctive composition.

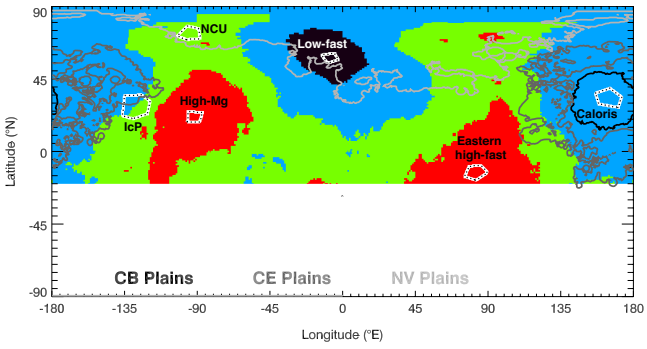

Fig. 3. Mercury's geochemical terrane map derived from the fast-neutron compositional map (Fig. 2); red, green, blue, and black represent different fast-neutron signatures. Labeled black/white contours outline the regions used for the simulations shown in Fig. 1. Contours (solid lines) show the mapped boundaries of the Caloris basin interior plains (CB), Caloris exterior plains (CE), and northern volcanic plains (NV) [17] .

References: [1] L.G. Evans et al., *JGR*, 117, E00L07, 2012; [2] L.G. Evans et al., *Icarus*, 257, 417, 2015; [3] D.J. Lawrence et al., *Science*, 339, 292, 2013; [4] L.R. Nittler, et al., *Science*, 333, 1847, 2011; [5] P.N. Peplowski et al., *Science*, 333, 1850, 2011; [6] P.N. Peplowski et al., *JGR*, 117, E00L04, 2012; [7] P.N. Peplowski et al., *JGR*, 117, E00L10, 2012; [8] P.N. Peplowski et al., *Icarus*, 228, 86, 2014; [9] R.D. Starr et al., *JGR*, 117, E00L02, 2012; [10] S.Z. Weider et al., *JGR*, 117, E00L05, 2012; [11] S.Z. Weider et al., *Icarus*, 235, 170, 2014; [12] S.Z. Weider et al., *EPSL*, 416, 109, 2015; [13] P.N. Peplowski et al., *Icarus*, 253, 346, 2015; [14] K.R. Stockstill-Cahill et al., *JGR*, 117, E00L15, 2012; [15] O. Gasnault et al., *GRL*, 28, 3797, 2001; [16] A.W. Beck et al., *MAPS*, 50, 1311, 2015; [17] B.W. Denevi et al., *JGR Planets*, 118, 891, 2013; [18] C.M. Ernst et al., *LPS*, this meeting, 2016.

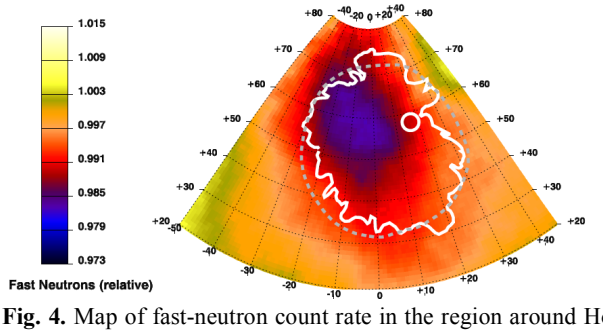

Fig. 4. Map of fast-neutron count rate in the region around Hokusai crater (white circle) and its ejecta (white trace). Dashed gray line shows the outline of this ejecta deposit after being smoothed by the fast-neutron response.